

## MODELING OF EDGE RECOMBINATION LOSSES IN HALF-CELLS

A. Fell<sup>1</sup>, H. Sträter<sup>2</sup>, M. Müller<sup>2,3</sup>, H. Steinkemper<sup>1</sup>, J. Schön<sup>1,4</sup>, M. Hermle<sup>1</sup>, M. C. Schubert<sup>1</sup>, D. H. Neuhaus<sup>2</sup> and S. W. Glunz<sup>1,4</sup>

<sup>1</sup>Fraunhofer Institute for Solar Energy Systems, Freiburg, Germany

<sup>2</sup>Solarworld Innovations, Freiburg, Germany

<sup>3</sup>now with TU Bergakademie Freiberg, Institute of Applied Physics, Freiberg, Germany

<sup>4</sup>Department of Sustainable Systems Engineering (INATECH), Albert Ludwigs University Freiburg, Freiburg, Germany

**ABSTRACT:** A new approach to model the impact of edge recombination within silicon solar cells using a 3D simulation of the entire cell geometry within Quokka3 is presented. The contribution of edge recombination within the space charge region (SCR), which is not directly accounted for in Quokka3's skin concept, is included by an effective property, a localized edge-length specific saturation current density with an ideality factor of 2:  $J_{02,edge}$ . A worst-case value of 19 nA/cm was found to be largely invariable for varying device properties. The new model is applied to predict the worst-case influence of the cut-edge within PERC half-cells. A moderate efficiency loss of 0.1 %<sub>abs</sub> is predicted, for which the SCR and non-SCR edge recombination contribute non-additive. Differentiating those two loss mechanisms reveals a very similar impact on light-JV characteristics dominantly on pseudo-fill-factor, whereas only the SCR mechanism is visible in dark-JV curves as an increased  $J_{02}$ . This means that non-SCR edge loss contributions will be missed by the commonly applied dark- $J_{02}$  characterization approach. Dedicated experiments to reveal the different mechanisms by measuring front and rear laser-scribed half-cell designs before cleavage are carried out and compared to the simulations results.

Keywords: simulation, modelling, silicon solar cell, edge loss

## 1 INTRODUCTION

The use of half-cells for higher module efficiency is becoming an increasingly popular topic both in research [1,2] and industry [3,4]. Its main advantage is related to lower ohmic interconnection losses, increasing mainly the fill factor and subsequently the power of the module considerably. However, the efficiency of the individual cells can be adversely affected, due to imperfections at the cut-edge, and an overall higher edge-to-area ratio. Two main loss mechanisms both originating from a high surface recombination at the cell edges are differentiated: i) recombination at the main part of the bulk which can be assumed quasi-neutral (qn), and ii) in the case the pn-junction extends right to the edge, additionally recombination in the space-charge-region (SCR) [5]. A quantitative understanding and differentiation via suitable characterization methods of those loss mechanisms is important when designing and optimizing half-cells.

Previous work on modeling and characterizing losses due to cut edges did commonly use an external diode model, where an increase of the second diode  $J_{02}$  was attributed to the entire edge losses, motivated by the SCR recombination theory having an ideality of 2 [5–9]. This paper aims to differentiate the contributions within and outside of the SCR by modeling and experiments.

In a first modeling step, Sentauros Device [10] simulations of a 2D edge domain are performed. The same domain is subsequently setup in Quokka3 [11], and validated against the Sentauros simulations. For this, Quokka3 supports an edge-length specific saturation current density with an ideality factor of 2,  $J_{02,edge}$ , localized at the edges, to represent SCR recombination, see [12] for details. Then Quokka3 is used to simulate the entire half-cell geometry in a single 3D domain, including metal resistance, to straightforward and accurately model the (measurable) influence of the edge region on the cell characteristics. Finally, half-cell layouts are cut with different conditions at Solar World Innovations (SWIN), and IV-results are compared to the simulations.

## 2 MODELING

The cell design and device properties for all simulations are based on the PERC cell in [13].

### 2.1 2D edge domain

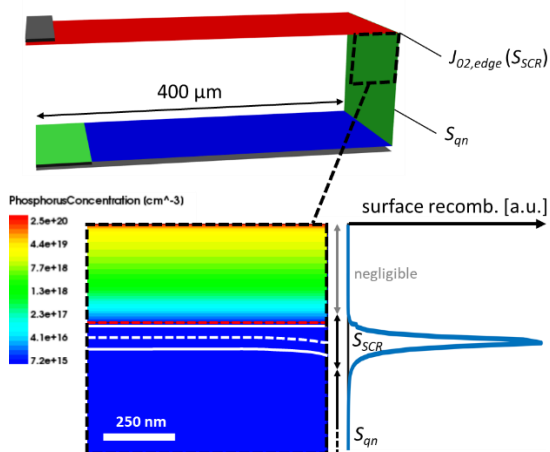


**Figure 1:** Sketch of the 2D edge solution domain; *upper*: overview as produced by Quokka3; *lower*: corner region as produced by Sentauros, showing the phosphorus concentration (colorplot), metallurgical junction depth (red dotted line), SCR (white lines, dotted line corresponds to equal carrier densities), and exemplary extracted surface recombination rate along the edge.

In Figure 1 the geometry of the 2D edge domain, representing a small stripe including the cut-edge, is shown. The same domain is setup in Sentauros Device as well in Quokka3. In Sentauros, surface recombination in the SCR,  $S_{SCR}$ , can be set independently of the other surface recombination at the quasi-neutral part of the bulk edge,  $S_{qn}$ , by defining a small separate surface region around the pn-junction. Due to the conductive boundary approach in Quokka3, the SCR is not directly modeled and therefore  $S_{SCR}$  cannot be directly defined. Rather a local edge-length

specific  $J_{02,edge}$  at a small region at the edge is applied, representing SCR recombination commonly known to show an ideality factor of 2. The absolute value of  $J_{02,edge}$  is not known a-priori for a given  $S_{SCR}$ , but fitted to the Sentaurus simulation results.

### 2.2 3D half-cell domain

To accurately model the influence of the edge on the half-cell performance, the recent performance boost through Quokka3 is used to discretize and solve the entire cell geometry in 3D, see Figure 2. The domain includes the metal current transport, fully accounting for its distributed nature.

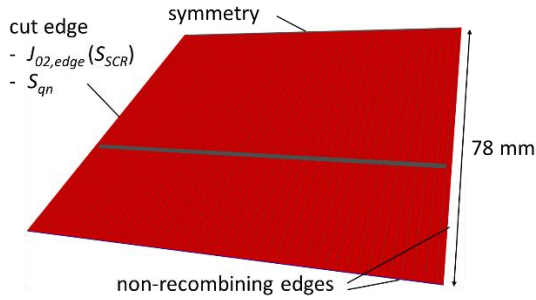


**Figure 2:** (Half of a) half-cell solution domain as defined in Quokka3. The entire geometry is discretized in 3D (including the bulk thickness) and solved, accurately quantifying the influence of the cut-edge properties on the cell characteristics.

## 3 EXPERIMENTAL

For validation of the modeled differences in edge recombination multicrystalline Al-BSF solar cells are prepared with a half cell metallization layout comprising neither front nor rear paste laydown in the half cell region where the laser scribing process takes place to prevent molten metallization. The laser scribing process is carried out with an IR disc laser from front and rear side, respectively. After scribing the cells effectively represent half-cells for which in the case of front scribing high additional SCR recombination is to be expected, whereas for rear scribing only additional non-SCR recombination is introduced. The half cells are obtained by mechanical cleavage.

The solar cells are characterized for their light and dark current-voltage characteristics with a standard HALM IV-tester measuring in a hysteresis-free setup. The calibration of short-circuit current  $I_{SC}$  for the half cells is carried out by defining  $I_{SC}$  of the full cells similar to the sum of  $I_{SC}$  of the two corresponding half cells. This approach is supported by the simulation results showing negligible  $I_{SC}$  losses due to edge recombination. The calibration is averaged for three full cells and their six half cells. The electrical characterization is carried out before laser scribing, after laser scribing and after mechanical cleavage.

## 4 RESULTS AND DISCUSSION

For a worst-case scenario, assuming surface recombination velocities at the limit of thermal velocity  $S_n = S_p = 10^7$  cm/s, a value of  $J_{02,edge} = 19$  nA/cm within Quokka3 provides good agreement to the Sentaurus simulations. In [12] it was found by a substantial variation of device properties that it in fact states a largely invariable

value, thus valid for any pn-junction bordering a highly recombining edge within (typical) silicon solar cells. Having such a fundamentally valid  $J_{02,edge}$  value, makes the consideration of SCR edge losses within Quokka3 particularly straightforward, as the Sentaurus fits do not have to be redone for varying device properties.

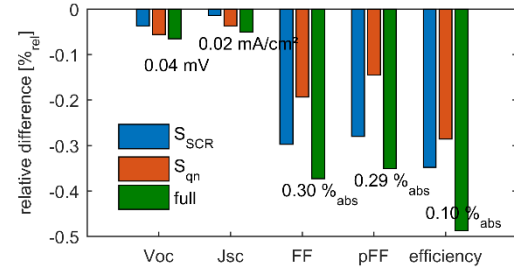


**Figure 3:** Simulated change of main light-JV parameters of the PERC half-cell due to different edge recombination cases, compared to the reference case without edge recombination; inserted values denote the absolute loss for the case of full edge recombination.

In Figure 3, simulated losses of light-JV parameters of the half-cell for three worst-cases are shown, relative to the case of no edge recombination: a)  $S_{SCR} = 10^7$  cm/s, b)  $S_{qn} = 10^7$  cm/s, c)  $S_{qn} = S_{SCR} = 10^7$  cm/s. It can be seen that both loss mechanisms mainly influence  $pFF$  and show similar absolute impact on efficiency for this worst-case example. They are not additive, which is due to the transport of minority carriers to the neighboring recombination regions being limited by diffusion. Overall, a moderate worst-case efficiency loss due to cut-edge recombination of 0.1 %<sub>abs</sub> is predicted.

Looking at the simulated dark-JV's in Figure 4, it can be seen that despite both loss mechanisms introducing similar non-idealities in the light-JV, solely the SCR loss contribution is visible as a non-ideality in the dark-JV. This means that an experimental determination of edge losses via the commonly applied  $J_{02}$  extraction from dark JV-curves is not generally sufficient: for the case that non-SCR edge recombination dominates, a possibly significant loss for light-JV performance is missed.

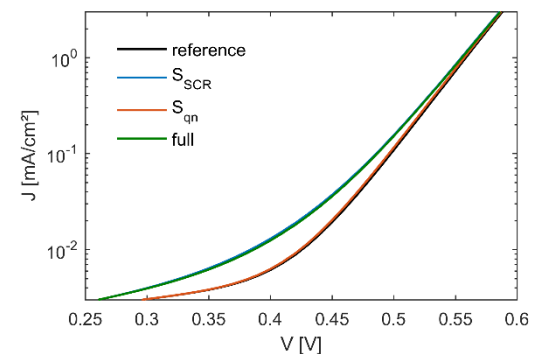


**Figure 4:** Simulated dark JV-curves of the PERC half-cell for the different edge loss cases; a typical external shunt resistance of  $10^5 \Omega\text{cm}^2$  is assumed

In Figure 5 the experimental results for  $V_{oc}$ ,  $FF$  and (dark-)  $J_{02}$  are shown for the two different cut conditions (front and rear side), before cleavage of the cell. As expected in both cases no notable impact on  $V_{oc}$  is observed. The loss for front scribing is even larger than predicted by the worst-case simulations, meaning that the laser did likely introduce damage to the SCR extending some distance into the

material, or lead to surface area enlargement due to a non-clean cut. The  $FF$  loss due to rear-scribing is well comparable with the  $S_{qn}$  simulations, the apparent increase of  $J_{02}$  is however statistically not significant, and does not allow to prove or disprove the dark-JV simulation results. Improved experiments on a PERC design have been started but were not finished by the time of the conference.

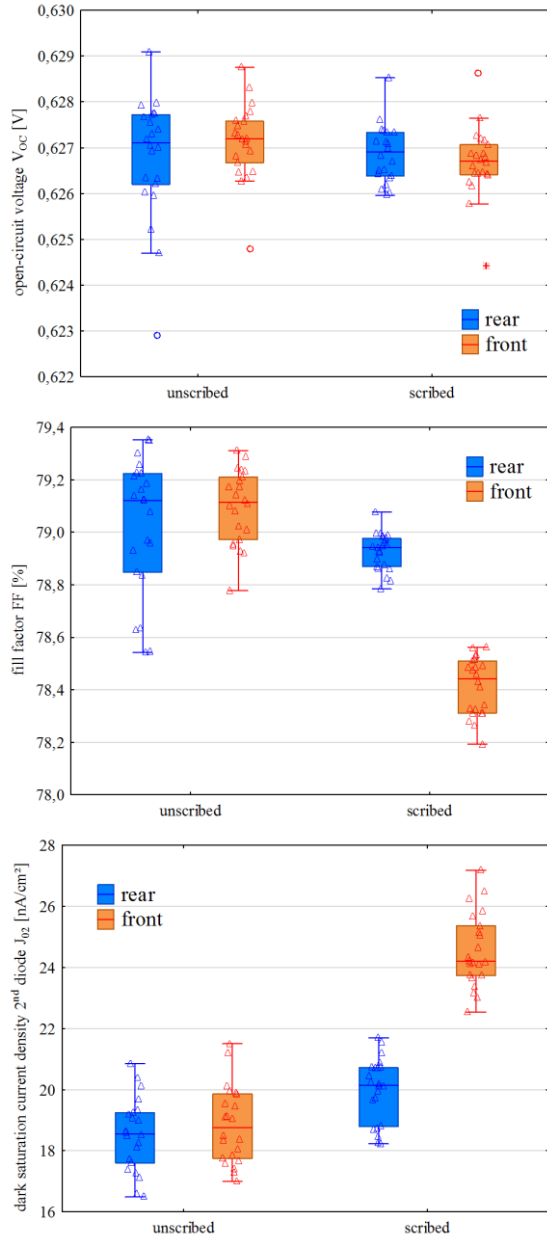


**Figure 4:**  $V_{oc}$ ,  $FF$  and  $J_{02}$  (from dark-JV) of the experimental cells before and after laser scribing from front and rear side.

## 5 CONCLUSIONS

A largely invariable localized  $J_{02,edge}$  value of 19 nA/cm was found to well represent worst-case SCR edge recombination within Quokka3's skin concept. It is applied to accurately predict the worst-case influence of the cut-edge within PERC half-cells, by simulating the entire cell geometry in 3D. A moderate efficiency loss of 0.1 %<sub>abs</sub> is predicted, for which the SCR and non-SCR edge

recombination contribute non-additive. Differentiating those two loss mechanisms reveals a very similar impact on light-JV characteristics dominantly on  $pFF$ , whereas only the SCR mechanism is visible in dark-JV curves as an increased  $J_{02}$ . This is important for the experimental characterization of edge losses, which is commonly carried out by determining the increase of dark  $J_{02}$ : for a case where non-SCR recombination dominates, e.g. by edge design changes to suppress SCR recombination, this common characterization approach misses potentially significant edge losses.

Dedicated experiments to reveal the different mechanisms by measuring front and rear laser-scribed half-cell designs before cleavage were carried out. The front laser scribing (through the emitter) reveals  $J_{02}$  increase beyond the simulated worst-case, indicating increased recombination due to laser damage extending into the material or surface area enlargement. The non-SCR losses show a  $FF$  loss similar as predicted by the simulations, other trends are however not statistically relevant to prove or disprove the simulations. Refined experiments are under way.

## ACKNOWLEDGEMENTS

This work was financially supported by the German Federal Ministry for Economic Affairs and Energy (BMWi) within the research project "PVBat400" under Contract No. 0324145.

The authors thank Nico Wöhrle (Fraunhofer ISE) for thorough beta-testing of the edge loss implementation in Quokka3.

Andreas Fell acknowledges funding by the European Commission through the Marie-Curie fellowship "Quokka maturation".

## REFERENCES

- [1] S. Eiternick, F. Kaule, H.-U. Zühlke, T. Kießling, M. Grimm, S. Schoenfelder, M. Turek, High Quality Half-cell Processing Using Thermal Laser Separation, *Energy Procedia* 77 (2015) 340–345.
- [2] R. Witteck, D. Hinken, H. Schulte-Huxel, M.R. Vogt, J. Müller, S. Blankemeyer, M. Köntges, K. Bothe, R. Brendel, Optimized Interconnection of Passivated Emitter and Rear Cells by Experimentally Verified Modeling, *IEEE Journal of Photovoltaics* 6 (2) (2016) 432–439.
- [3] C. Arndt, D. Stichtenoth, N. Müller, M. Reinicke, D. Grote, U. Schröder, M. Scherr, M. Weser, F. Lange, P. Voigt (Eds.), *Manufacturing of 300Wp Modules by Industrialization of PERC Solar Cell Technology Including Crystal, Cell and Module Development*, 2014.
- [4] S. Zhang, X. Pan, H. Jiao, W. Deng, J. Xu, Y. Chen, P.P. Altermatt, Z. Feng, P.J. Verlinden, 335-W World-Record p-Type Monocrystalline Module With 20.6% Efficient PERC Solar Cells, *IEEE Journal of Photovoltaics* 6 (1) (2016) 145–152.
- [5] R. Kuhn, P. Fath, E. Bucher (Eds.), Effects of pn-junctions bordering on surfaces investigated by means of 2D-modeling. Conference Record of the Twenty-Eighth IEEE Photovoltaic Specialists Conference - 2000 (Cat. No.00CH37036), 2000.
- [6] M. Hermle, J. Dicker, W. Warta, S.W. Glunz, G. Willeke (Eds.), Analysis of edge recombination for

- high-efficiency solar cells at low illumination densities, IEEE, 2003.
- [7] C. Chan, M. Abbott, B. Hallam, M. Juhl, D. Lin, Z. Li, Y. Li, J. Rodriguez, S. Wenham, Edge isolation of solar cells using laser doping, *Solar Energy Materials and Solar Cells* 132 (2015) 535–543.
  - [8] K. Rühle, M.K. Juhl, M.D. Abbott, L.M. Reindl, M. Kasemann, Impact of Edge Recombination in Small-Area Solar Cells with Emitter Windows, *IEEE Journal of Photovoltaics* 5 (4) (2015) 1067–1073.
  - [9] D. Bertrand, S. Manuel, M. Pirot, A. Kaminski-Cachopo, Y. Veschetti, Modeling of Edge Losses in Al-BSF Silicon Solar Cells, *IEEE Journal of Photovoltaics* 7 (1) (2017) 78–84.
  - [10] Synopsis, Sentaurus Device User Guide, release I-2013.12, Zurich, Switzerland, 2013.
  - [11] A. Fell, J. Schön, M.C. Schubert, S.W. Glunz, The concept of skins for silicon solar cell modeling, *Solar Energy Materials and Solar Cells* (2017).
  - [12] A. Fell, J. Schön, M. Müller, M.C. Schubert, S.W. Glunz, Modelling edge recombination in silicon solar cells, submitted to *IEEE Journal of Photovoltaics* (2017).
  - [13] A. Fell, K.R. McIntosh, P.P. Altermatt, G.J.M. Janssen, R. Stangl, A. Ho-Baillie, H. Steinkemper, J. Greulich, M. Müller, M. Byungsul, K.C. Fong, M. Hermle, I.G. Romijn, M.D. Abbott, Input Parameters for the Simulation of Silicon Solar Cells in 2014, *IEEE Journal of Photovoltaics* 5 (4) (2015) 1250–1263.